JOURNAL OF CATALYSIS 90, 75–83 (1984)

Strong Metal–Support Interaction in Ni/TiO_2: Auger and Vibrational Spectroscopy Evidence for the Segregation of TiO_x ($x \simeq 1$) on Ni and Its Effects on CO Chemisorption

SHINICHIRO TAKATANI AND YIP-WAH CHUNG

Department of Materials Science and Engineering, Northwestern University, Evanston, Illinois 60201

Received April 20, 1984; revised June 18, 1984

Auger electron spectroscopy (AES) and high-resolution electron energy loss spectroscopy (HREELS) showed that hydrogen reduction at 700°K of a 120-Å nickel film deposited on TiO_2 results in the segregation of TiO_x (x close to 1) onto the nickel surface. Titanium oxide appears to diffuse rapidly through nickel. Room-temperature CO uptake was found to decrease with increasing surface titanium oxide concentration. HREELS showed that the concentration of bridge-bonded CO relative to on-top CO after room-temperature CO exposure decreases with increasing titanium oxide coverage on nickel. A site giving rise to a CO stretching frequency of 1850 cm^{-1} was found to survive after extended reduction. This was attributed to a site near the surface titanium oxide on nickel. The present study suggests that both physical coverage of the nickel surface by TiO_x and the chemical interaction between nickel and TiO_x on the surface are involved in SMSI.

1. INTRODUCTION

The pioneering work of Tauster *et al.* (*1*) has stimulated numerous studies of the strong effects of titania support on the chemisorption and catalytic properties of group VIII metals. These effects were attributed to the existence of a strong metal–support interaction (SMSI). The main features of SMSI are the suppression of CO and hydrogen sorption capacity of metals (*1, 2*) and radical changes in activity and selectivity in catalytic reactions such as CO hydrogenation (*3*).

Considerable efforts have been made to elucidate the mechanism of SMSI (*4–15*). In the charge transfer model (*4*), it was proposed that the interaction occurs through charge transfer (bonding) between the metal and the titania support. Recent work by Dumesic and co-workers (*12*) on Fe/titania showed that SMSI behavior persists even for iron particles with diameter exceeding 200 Å. Charge transfer from one phase to another cannot explain this observation because the excess charge would be screened out over a distance on the order of atomic spacing. They proposed that during high-temperature reduction to induce SMSI, titania diffuses to the metal surface. In subsequent work by Dumesic and co-workers (*13*), the hydrogen uptake behavior on several metals supported on titania was also discussed in terms of the presence of titanium oxide species on metal surfaces. Resasco and Haller (*14*) found that the ethane hydrogenolysis activity of Rh/titania follows a square-foot dependence on the reduction time, strongly suggesting the operation of a diffusion-controlled mechanism.

In addition to the numerous studies on high-surface-area metal catalysts, several attempts were made to study low-surface-area (~1 cm^2) model SMSI specimens using ultrahigh vacuum and surface science techniques. Chung and co-workers demonstrated that about 5–6 Å of nickel vapor deposited onto single crystal TiO_2 shows SMSI behavior (*8*). They further showed that a Ni(111) single crystal partially covered with reduced titania shows essentially the same CO hydrogenation kinetics and product distribution as those of SMSI catalysts (*15*). Both studies support the model

0021-9517/84 $3.00

proposed by Dumesic and co-workers. There is some early evidence from the photoemission work of Kao *et al.* (*7*) that there is rapid interdiffusion between Ni and TiO_2 at temperatures as low as 300°C. Recent work by Cairns *et al.* (*16*) using nuclear backscattering also confirmed this finding.

In the present paper, we report Auger electron spectroscopy (AES) and high-resolution electron energy loss spectroscopy (HREELS) investigation on Ni/TiO_2. Both techniques clearly demonstrate the segregation of reduced titanium oxide on the nickel surface after hydrogen reduction at 700°K. HREELS provides further insight into the nature of the surface titaium oxide and its effects on CO chemisorption on nickel.

2. EXPERIMENTAL SECTION

Auger studies were done in a Physical Electronics PHI 590A ultrahigh vacuum scanning Auger microprobe (SAM). The titanium specimen used in this study is a 1-cm^2 0.004-in.-thick polycrystalline foil purged of bulk impurities by a series of sputtering and annealing cycles. A titanium oxide film was formed on the titanium foil surface by heating to 673°K under 3×10^{-6} Torr oxygen for 5 min, followed by deposition of 120-Å-thick nickel layer at the rate of 10 Å/min. The specimen temperature rose to no more than 330°K during Ni evaporation. The resulting Ni/titania specimen was then reduced at 700°K under 1×10^{-6} Torr hydrogen for various amounts of time. After the reduction, Auger profiles of Ni, Ti, and O were determined by sequential argon ion sputtering and Auger analysis at room temperature. The carbon monoxide uptake at room temperature was measured from the carbon Auger intensity after exposing the specimen to 100L CO. In both cases, Auger measurements were made by rastering a 2-kV/100-nA electron beam over a 0.5- × 0.5-mm area at 30 frames/sec to minimize electron beam effects.

HREELS studies were done in another ultrahigh vacuum chamber equipped also with an Auger spectrometer and other facilities for specimen preparation. The HREELS spectrometer used is similar to the one developed by Ibach (*17*) and modified by Sexton (*18*). The electron beam was set at 1 eV primary energy and an angle of incidence of 60°. Scattered electrons were collected in the specular direction. The specimen for HREELS work was prepared in the same manner as described above.

3. RESULTS

3.1. Auger Electron Spectroscopy Results

Under our oxidation conditions, we measured an Auger O(510 eV)/Ti(385 eV) peak ratio of 1.6–1.7 for the oxidized titanium surface. This is close to that from bulk TiO_2. Ti(385 eV) and Ti(415 eV) Auger peaks show shapes characteristic of TiO_2 (*19*). It is therefore concluded that a near-stoichiometric TiO_2 layer was formed with thickness exceeding the escape depth of Auge electrons.

Auger intensities of Ti(385 eV) and O(510 eV) as a function of reduction time are shown in Fig. 1. The Ti and O Auger intensities increased with reduction time. For example, after 36 min of reduction, the Ti Auger intensity increased from approximately zero to about 25% of the Auger intensity from bulk TiO_2. The O/Ti Auger in-

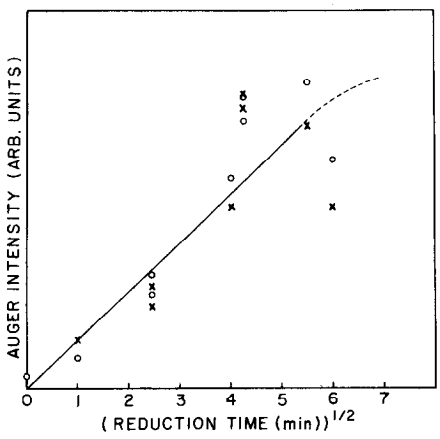

FIG. 1. Auger intensity of Ti(o) and O(x) at 385 and 510 eV, respectively, as a function of reduction time.

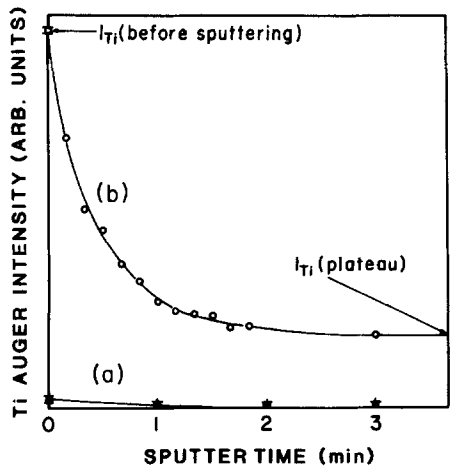

FIG. 2. Sputter profiles of Ti Auger intensity from Ni/titania (a) before reduction, (b) after 18 min of reduction at 700°K.

tensity ratio was between 0.8 and 1.0 after 5 to 36 min of reduction.

Sputter-profiles of Ti(385 eV) Auger intensity from the Ni/titania specimen without reduction and after 18 min of reduction at 700°K are shown in Figs. 2a and b. The sputter rate was approximately 5 Å/min. The Ti Auger intensity from the specimen without reduction was negligible during the initial several minutes of sputtering. On the other hand, after reduction at 700°K, enrichment of Ti on the surface was clearly observed. The Ti signal was seen to decrease from I_{Ti} (before sputtering) on the surface to a steady state value I_{Ti} (plateau) (Fig. 2b) after 1 to 2 min of sputtering. Both I_{Ti} (before sputtering) and I_{Ti} (plateau) depend on the reduction time. Oxygen was found to have a profile similar to that of titanium.

Room-temperature CO uptake of the Ni/Titania specimen was found to decrease monotonically with increasing reduction time at 700°K as shown in Fig. 3.

3.2. High-Resolution Electron Energy Loss Spectroscopy Results

Figure 4 is the ELS spectrum of a titanium foil freshly oxidized under 3×10^{-6} Torr oxygen at 673°K for 5 min taken prior to the nickel deposition. It shows loss peaks at 440, 790, 1580, and 2380 cm^{-1}. Further oxidation increases the intensities of the loss peaks while the frequencies remain unchanged. For example, the 790-cm^{-1} peak to elastic peak intensity ratio increases by 40% after 20 min of oxidation.

Figure 5 shows ELS spectra of Ni/titania taken after the specimen was reduced at 700°K under 1×10^{-6} Torr hydrogen for various amounts of time followed by 100L CO exposure at room temperature. The loss bands at higher energies are due to CO stretching modes. There are two major losses at 1910 cm^{-1} (bridge-bonded CO) and 2020 cm^{-1} (on-top CO) (*20–23*). With increasing reduction time, the intensity due to bridge-bonded CO decreases more rapidly than that of the on-top CO. A loss peak

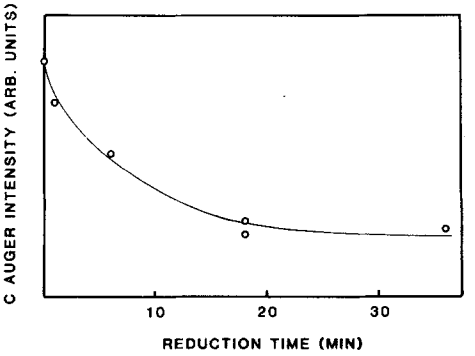

FIG. 3. Room-temperature CO uptake by Ni/titania as a function of reduction time at 700°K.

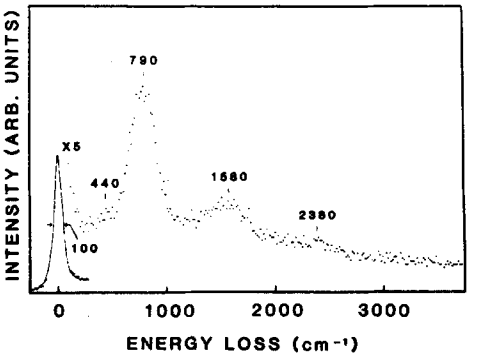

FIG. 4. Energy loss spectrum of titanium foil oxidized under 3×10^{-6} Torr O_2 at 673°K for 5 min.

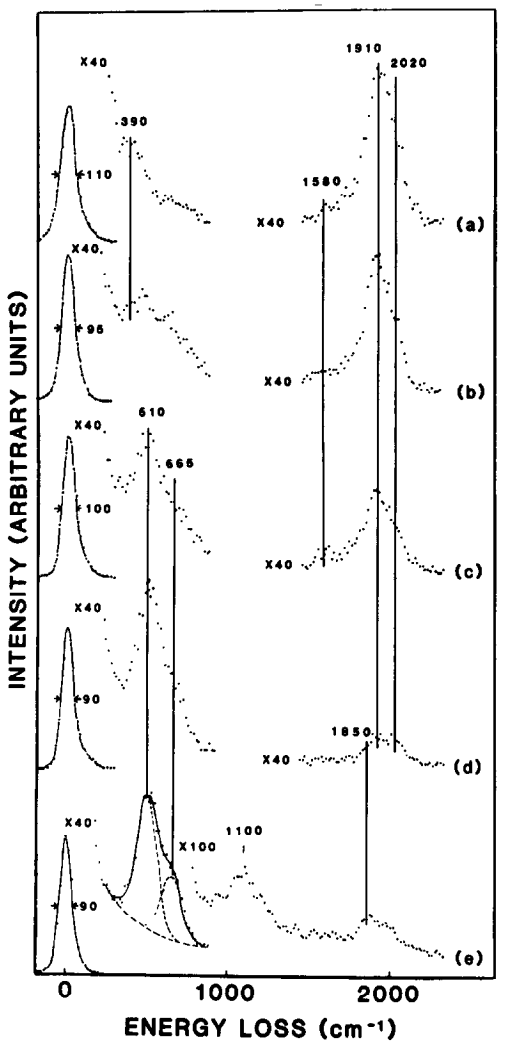

FIG. 5. Energy loss spectra of Ni/titania after 100L CO exposure at room temperature: (a) specimen reduced for 1 min, (b) 6 min, (c) 16 min, (d) 36 min, (e) 64 min.

around 1580 cm^{-1} was observed initially (Figs. 5a–c), but was absent after longer reduction time (Figs. 5d–e). After 64 min reduction, a new CO stretching loss feature becomes apparent at 1850 cm^{-1} (Fig. 5e).

In the lower energy region, a loss at 390 cm^{-1} was observed after CO exposure on the specimen after a brief reduction (Fig. 5a). With increasing reduction time, new peaks at 510 and 665 cm^{-1} evolved and dominated in this energy region (Figs. 5c–e). In addition, a loss feature around 1100 cm^{-1} (Fig. 5e) was found to grow with further reduction. These losses (510, 665, 1100 cm^{-1}) were present before CO exposure.

For the purpose of interpretation of some loss peaks at lower energies in Fig. 5, an ELS spectrum of a sputter-annealed titanium foil exposed to 2L oxygen at room temperature is presented in Fig. 6. Least-square fitting of the major loss band using three Gaussians resulted in a strong peak at 530 cm^{-1} and shoulders at 415 and 665 cm^{-1}. The losses around 970 cm^{-1} often appeared even before oxygen exposure. Auger spectra of such surfaces showed a weak oxygen signal.

4. DISCUSSION

4.1. AES Results

Evolution of titanium and oxygen Auger signals on the Ni/titania surface after reduction shown in Fig. 1 and typical sputter profiles shown in Fig. 2b indicate clearly the segregation of titanium and oxygen on the nickel surface after reduction at 700°K. The initial decrease of the Ti Auger signal in the sputter profile is not an artifact due to preferential sputtering. It is known that the sputter yield of metallic titanium by 2-kV argon ions is about half of that of metallic nickel (*24*), and for titanium in the oxide form, the sputter yield is even smaller (*25*). Therefore, the trend in the sputter profile in Fig. 2b is opposite to what is expected from

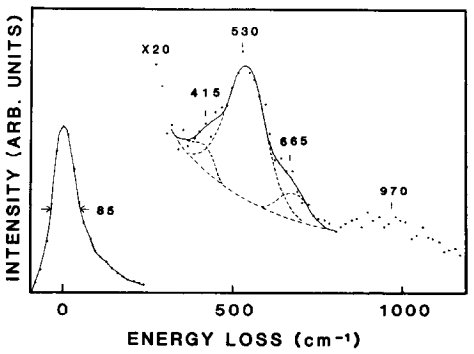

FIG. 6. Energy loss spectrum of titanium foil exposed to 2L O_2 at room temperature.

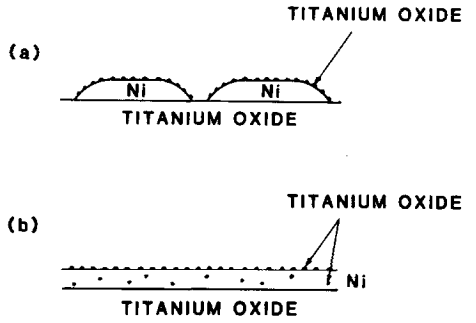

FIG. 7. Two models of Ni/titania specimen after reduction.

preferential sputtering between nickel and titanium or titanium oxide.

The nearly linear dependence of the Ti and O Auger intensity on the square root of reduction time is indicative of a diffusion-controlled process through which surface titanium and oxygen species are derived.

An O/Ti Auger intensity ratio of 0.8–1.0 on the surface indicates an O/Ti atomic ratio of 1.0–1.25. We also observed that the Ti(385 eV) and Ti(415 eV) Auger peak shapes are close to those in TiO (*19*). Considering also the large heat of formation of titanium oxide compared to that of nickel oxide, it is probably the case that surface oxygen is associated mainly with titanium forming TiO_x with x close to 1. In the following, we will call this "titanium oxide."

To determine the surface titanium coverage from the sputter profile, one can consider two extreme models of the Ni/titania specimen after reduction at 700°K as illustrated in Figs. 7a and b. In Fig. 7a, the nickel is assumed to form islands on the titania substrate, and the nickel surface is partially covered with titanium oxide. The plateau in the sputter profile (Fig. 2b) is therefore due to titanium signal from the substrate through openings in the nickel layer. Therefore, one can estimate the surface titanium concentration θ_{Titanium} from the equation

$$\theta_{\text{Titanium}} = \frac{1}{k}\left[I_{\text{Ti}}\ (\text{before sputtering}) - I_{\text{Ti}}\ (\text{plateau})\right] \quad (1)$$

where k is the titanium Auger intensity from one monolayer of TiO_2.[1] In the other model as illustrated by Fig. 7b, the nickel layer is assumed to cover uniformly the substrate and a small amount of titanium oxide is dissolved in nickel. The finite Ti Auger intensity in the plateau is therefore due to titanium oxide dissolved in nickel. Assuming homogeneous distribution of titanium oxide within the nickel layer except on the surface, one can show the surface titanium concentration θ_{Titanium} in the equation

$$\theta_{\text{Titanium}} = \frac{1}{k}\left[I_{\text{Ti}}\ (\text{before sputtering}) - \alpha I_{\text{Ti}}\ (\text{plateau})\right] \quad (2)$$

where $\alpha = \exp(-d/\lambda \cos\varphi)$ with $d = 3.2$ Å, $\lambda = 9$ Å, and $\varphi = 42.3°$. Typically, I_{Ti} (plateau) is not more than 20% of I_{Ti} (before sputtering). Therefore, we expect these two models to give similar prediction of θ_{Titanium}. From Eqs. (1) and (2), together with the corresponding CO uptake information (Fig. 3), we obtained normalized plots of CO uptake versus surface titanium concentration as shown in Fig. 8 by (o) for model a and (x) for model b. The overall feature is essentially the same for both models. The θ_{CO} decreases rapidly with increasing θ_{Titanium}. From the initial slope of the curve, one can show that one titanium atom deactivates approximately five to six surface nickel atoms for CO adsorption. The room-temperature CO uptake appears to level off to about 30% the prereduction value as seen in Fig. 8, in close agreement with the earlier finding of Smith *et al.* (*2*) on high-surface-area Ni/titania catalysts and the single crystal work of Kao *et al.* (*26*).

Data in Figs. 1 and 2 show that titanium oxide diffuses fairly rapidly through the Ni

[1] The k in the text is estimated by $k = I_{\text{Ti}}$ (thick oxide) $\cdot (1 - \alpha)$, $\alpha = \exp(-d/\lambda \cos\varphi)$, where I_{Ti} (thick oxide) is Ti Auger intensity from a thick oxide layer formed on the Ti foil, d the spacing of layers, λ mean free path, and φ collection angle, We assumed $d = 3.2$ Å, the layer spacing of single crystal TiO_2, $\lambda = 9$ Å and $\varphi = 42.3°$.

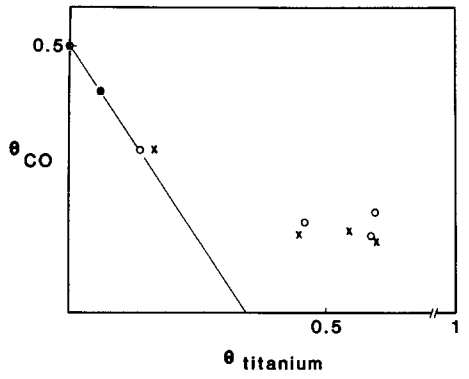

FIG. 8. Room-temperature CO uptake versus Ti coverage on the Ni surface based on model a (o), and model b (x) illustrated in Fig. 7. The $\theta_{\text{titanium}} = 1$ corresponds to $1 \times 10^{15}/\text{cm}^2$, the packing density of Ti on TiO_2 (110). The $\theta_{CO} = 0.5$ corresponds to the saturation coverage of CO on Ni(111).

film, presumably through grain boundaries and other imperfections. A rough estimate can be made of the diffusion coefficient D as follows. A substantial amount of titanium oxide appears on the nickel surface (thickness 120 Å) after about 1000 sec. From the equation $l^2 = 2Dt$, where l is the diffusion distance (120 Å) and t is the diffusion time (1000 sec), D was found to be 7.2×10^{-16} cm²/sec at 700°K. Kao *et al.* (*8*) found that $D(573°\text{K}) \simeq 2 \times 10^{-17}$ cm²/sec. From these data, the activation energy for such diffusion process is estimated to be around 23 kcal/mole.

4.2. *HREELS Results*

In the ELS spectrum of oxidized titanium surface before Ni deposition (Fig. 4), peaks at 790 and 440 cm^{-1} are close to surface phonon losses at 766 and 436 cm^{-1} observed on TiO_2(100) (*27*). One can assign the peaks at 1580 and 2380 cm^{-1} as double and triple excitations of the mode at 790 cm^{-1}. The 790-cm^{-1} loss to elastic peak intensity ratio in Fig. 4 was found to increase after prolonged oxidation under identical impact energy (1 eV) and geometry. This implies that the oxide layer formed under the present experimental conditions is thinner than the ELS probing depth, viz. $1/Q_\parallel$, when $1/Q_\parallel$ is the wavenumber of the surface wave characteristically excited by incident electrons through the dipole scattering mechanism (*28*). For electron excitation at 1 eV, one finds $Q_\parallel$ is approximately 40 Å. Therefore, we expect the oxide thickness to be somewhere between 15 Å (~Auger probing depth) and 40 Å (ELS probing depth).

Numerous vibrational studies of CO adsorption have been done on nickel single crystals. On Ni(111) and Ni(100), CO stretching mode for bridge-bonded CO was found at 1895–1930 cm^{-1} and on-top CO at 2045–2065 cm^{-1} with intensity and frequency dependent on the CO coverage (*20–22*). At low coverage, Ni(111) shows CO stretch at 1815–1845 cm^{-1} attributed to CO on threefold site (*22*). On Ni[5(111) × (1$\bar{1}$0)], on-top CO was found between 2010 and 2060 cm^{-1} and two- and threefold-bridge CO between 1820 and 1960 cm^{-1} (*23*). In addition, a CO stretch at 1510–1540 cm^{-1} was observed and attributed to CO on a step site (*23*). In the present study, we evaporated a nickel film onto a titania surface which was subsequently heated at 700°K in hydrogen. Major loss features due to CO stretch were observed at 1580, 1910, and 2020 cm^{-1} (Fig. 5). Comparing with literature data cited above, we assign the loss at 1910 cm^{-1} to bridge-bonded CO and 2020 cm^{-1} to on-top CO. The evaporated Ni film is expected to contain considerable steps or kinks so that the assignment of 1580 cm^{-1} to CO on step or kink site is reasonable. The 1580-cm^{-1} loss was found only after CO exposure and is therefore not due to water impurity. Heating at 700°K is expected to improve the ordering of the nickel film, thereby reducing step or kink density. This is consistent with the disappearance of the 1580-cm^{-1} peak after extended heating (Figs. 5d and e). It is unlikely that the peak at 1580 cm^{-1} is due to CO on a site associated with surface titanium oxide, since the peak is absent after extended reduction where the concentration of surface titanium oxide is higher.

The CO stretch loss intensity corre-

sponding to bridge-bonded CO decreases more rapidly with increasing reduction time than that of the on-top CO, as seen in Fig. 5. On-top CO to bridge-bonded CO intensity ratio is about twice the prereduction value after 36 min of reduction. This indicates the relative increase of on-top CO concentration compared with bridge-bonded CO. The trend is opposite to what one may expect if the heat treatment merely increases the area of ordered (111) face since it is known that bridge-bonded CO dominates over on-top CO at saturation coverage on Ni(111) (*21, 22*). This relative concentration increase of on-top CO can be explained by the incorporation of species inactive for CO adsorption. Since a twofold bridge site requires two adjacent nickel atoms, the concentration of bridge sites decreases more rapidly after the incorporation of inactive species than that of on-top sites, analogous to the ensemble effect observed in alloy systems (*29*). In the present case, since this trend parallels that of the concentration increase of surface titaium oxide, such inactive species should correspond to titanium oxide. It should be mentioned that in the room-temperature adsorption study of Tanaka and White on Pt dispersed on TiO_2 support using ir absorption spectroscopy (*30*), only on-top CO was observed on the specimen reduced at 400°C while on the specimen reduced at 200°C, both on-top and bridge-bonded CO were present. Similar observation was also made by Vannice *et al.* on Pt/TiO_2 (*31*).

In the ELS spectrum for the specimen reduced for 64 min (Fig. 5e), the CO stretching band shows frequencies as low as 1850 cm^{-1}. This is too low to be attributed to bridge-bonded CO (*22*). On Ni(111), a loss at 1815–1845 cm^{-1} was observed at a low CO coverage and was attributed to CO adsorbed on a threefold site (*22*). However, the assignment of the 1850-cm^{-1} loss observed here to CO on a threefold site is contradictory to the ensemble effect—that is, the loss intensity due to CO adsorbed on a threefold site relative to on-top or twofold sites should decrease with increasing reduction time, i.e., increasing titanium coverage. The observed trend is just opposite (see Figs. 5d and e). We believe that the 1850-cm^{-1} loss is due to CO adsorbed on a site near the surface titanium oxide. One can notice some similarity of the system studied here to catalysts containing metal oxide additives. A titanium oxide promoted Rh catalyst has been found by ir spectroscopy to show CO stretching bands at 1830 and 2035 cm^{-1} after room-temperature CO exposure (*32*). For catalysts containing oxophylic metal oxides such as manganese oxide as additives, Sachtler (*33*) proposed a model in which CO adsorbs in a tilted position near the metal additive ion as a result of the interaction between oxygen in CO and the metal ions. The carbon–oxygen bond in this case is expected to be weakened. It is known that the CO hydrogenation activity is greatly enhanced for Ni/titania in the SMSI state (*3*). The site giving rise to 1850 cm^{-1} CO may act as an important active site for this reaction.

Next, we turn our attention to the loss peaks at lower energy in Fig. 5. The loss at 395 cm^{-1} in Fig. 5a can be assigned to be due to Ni–C stretch since it has been observed around 400 cm^{-1} for CO on Ni(111) (*21, 23*). Increasing reduction time gives rise to loss peaks at 510, 665, and 1100 cm^{-1}. These peaks were present even before CO exposure. Considering the present Auger observation, these new peaks are undoubtedly due to oxygen and titanium on or near the nickel surface. The question is how titanium and oxygen are arranged on the nickel surface. Although a definite answer cannot be obtained from the present data, we have made some attempts in this direction as discussed below.

After 2L oxygen exposure at room temperature to a clean titanium foil with a (0001) texture, a strong peak appears at 530 cm^{-1} (Fig. 6). This peak is likely to be due to oxygen on a threefold site on a Ti(0001) surface. On the other hand, oxygen on a threefold site of Ni(111) gives a frequency

of 570–580 cm^{-1} (*28*). The loss at 510 cm^{-1} in Figs. 5c–e is close to the 530-cm^{-1} loss due to oxygen on titanium (Fig. 6) and therefore can be favorably assigned as oxygen associated with surface titanium. However, the interaction of oxygen with nickel cannot be totally excluded. More realistically, one can consider the situation where an oxygen atom sits on a threefold site where one or two nickel atoms are replaced by titanium. The frequencies of the modes can be easily estimated by the method described in Ref. (*28*) assuming that the mode at 530 cm^{-1} in Fig. 6 is due to oxygen on a threefold site of titanium. We found that all the modes fall between 500 and 560 cm^{-1}. Therefore, the involvement of any Ni–O bond cannot be discerned from here. In Fig. 5c–e, there is a shoulder at the high-energy side of the 510-cm^{-1} peak. The peak appears to be around 665 cm^{-1}. This compares well with the shoulder around 665 cm^{-1} in Fig. 6 for oxygen on titanium. Together with the Auger result that surface titanium appears to be in a non-zero oxidation state as well as thermodynamic considerations, we believe that the oxygen is associated mainly with titanium.

The broad loss feature around 1100 cm^{-1} in Fig. 5e can be attributed to subsurface oxygen diffused from the titania substrate. It is known that Ni(111) exposed to oxygen often shows additional peaks at 970 and 1125 cm^{-1} which can be related to subsurface oxygen, and the unusually high frequencies are rationalized as oxygen squeezed in the metal substrate (*28*).

We also made some preliminary work function change measurements of Ni/titania due to heating at 700°K in hydrogen and under vacuum using the retarding potential method. The primary motivation was to obtain additional information about the surface titanium oxide. The work function was found to remain constant within +/− 0.1 eV after reduction treatments. As implied from the assignment of vibrational loss peaks, oxygen seems to exist both above and below the surface. Therefore, the nearly constant work function can be rationalized by the cancellation of the additional dipole moments in opposite directions near the surface.

Finally, in order for the partial coverage of the nickel surface by reduced titanium oxide as demonstrated in this study to be energetically favorable, the interaction between reduced titanium oxide and the surface nickel has to exceed the large Coulomb energy required to remove titanium oxide molecules from the bulk oxide (*33*). It is likely that d electrons in Ti^{n+} ($n < 4$) are involved in these interactions. Therefore, SMSI involves not only physical coverage of the metal surface by titanium oxide, but also chemical interaction between the metal and titanium. The close proximity between nickel and titanium oxide[2] as a result of their strong interaction makes it possible for the two ends of the CO molecules to be activated by them simultaneously, giving rise to interesting chemisorption and catalytic behavior.

5. SUMMARY

Both Auger and HREELS showed directly the segregation of TiO_x (x close to 1) onto the nickel surface after hydrogen reduction at 700°K of a 120-Å nickel film deposited on titanium dioxide. Titanium oxide appears to diffuse very rapidly through nickel. Room-temperature CO uptake was found to decrease with increasing surface titanium oxide concentration on nickel. HREELS showed that the concentration of bridge-bonded CO relative to on-top CO after room-temperature CO exposure decreases with increasing titanium oxide coverage. A site on which CO adsorbs with a stretching frequency of 1850 cm^{-1} was found to survive after extended reduction. This was attributed to a site near the surface titanium oxide on nickel. The present studies strongly suggest that physical cov-

[2] The idea of Ni/TiO_x periphery sites was raised by Burch and Flambard Ref. (*34*). But the concept of oxide migration was not discussed by them.

erage of the nickel surface by reduced titanium oxide and the chemical interaction between nickel and titanium are the key elements of SMSI.

ACKNOWLEDGMENTS

Acknowledgment is made to the Donors of the Petroleum Research Fund, administered by the American Chemical Society, for support of this research. Some parts of this research were carried out in the Surface Science Facility of Northwestern University Materials Research Center which is supported by the National Science Foundation MRL Program DMR 82-16972. We thank Professor W. M. H. Sachtler for many illuminating discussions and for communicating to us Refs. (*32*) and (*33*) prior to their publication.

Note added in proof. Subsequent to the submission of this paper, we learned that several groups have arrived at the same conclusion on titanium oxide migration onto the metal surface. This includes PtTi work by Ross and Somorjai, Rh by White *et al.*, Ni by Dumesic *et al.*, Rh by Henrich *et al.*, and Pt by Gorte *et al.*

REFERENCES

1. Tauster, S. J., Fung, S. C., and Garten, R. L., *J. Amer. Chem. Soc.* **100,** 170 (1978).
2. Smith, J. S., Thrower, P. A., and Vannice, M. A., *J. Catal.* **68,** 270 (1981).
3. Vannice, M. A., and Garten, R. L., *J. Catal.* **56,** 236 (1979).
4. Horsley, J. A., *J. Amer. Chem. Soc.* **101,** 2870 (1979).
5. Chung, Y. W., and Weissbard, W. B., *Phys. Rev. B* **20,** 3456 (1979).
6. Bahl, M. K., Tsai, S. C., and Chung, Y. W., *Phys. Rev. B* **21,** 1344 (1980).
7. Kao, C. C., Tsai, S. C., Bahl, M. K., Chung, Y. W., and Lo, W. J., *Surf. Sci.* **95,** 1 (1980).
8. Kao, C. C., Tsai, S. C., and Chung, Y. W., *J. Catal.* **73,** 136 (1982).
9. Chien, S. H., Shelimov, B. N., Resasco, D. E., Lee, E. H., and Haller, G. L., *J. Catal.* **77,** 301 (1982).
10. Sexton, B. A., Hughes, A. E., and Foger, K., *J. Catal.* **77,** 85 (1982).
11. Huizinga, T., Van't Blik, H. F. J., Vis, J. C., and Prins, R., *Surf. Sci.* **135,** 580 (1983).
12. Santos, J., Phillips, J., and Dumesic, J. A., *J. Catal.* **81,** 147 (1983).
13. Jiang, X. Z., Hayden, T. F., and Dumesic, J. A., *J. Catal.* **83,** 168 (1983).
14. Resasco, D. E., and Haller, G. L., *J. Catal.* **82,** 279 (1983).
15. Chung, Y. W., Xiong, G., and Kao, C. C., *J. Catal.* **85,** 237 (1984).
16. Cairns, J. A., Baglin, J. E. E., Clark, G. J., and Ziegler, J. F., *J. Catal.* **83,** 301 (1983).
17. Froitzheim, H., and Ibach, H., *Z. Phys.* **269,** 17 (1974).
18. Sexton, B. A., *J. Vac. Sci. Technol.* **16,** 1033 (1979).
19. Davis, G. D., Natan, M., and Anderson, K. A., *Appl. Surf. Sci.* **15,** 321 (1983).
20. Anderson, S., *Solid State Commun.* **21,** 75 (1977).
21. Erley, W., Wagner, H., and Ibach, H., *Surf. Sci.* **80,** 612 (1979).
22. Campuzano, J. C., and Greenler, R. G., *Surf. Sci.* **83,** 301 (1979).
23. Erley, W., Ibach, H., Lehwald, S., and Wagner, H., *Surf. Sci.* **83,** 585 (1979).
24. Scherzer, B. M. U., Behrish, R., and Roth, J., "Proceedings, International Symposium on Plasma Wall Interaction, Oct. 1976," p. 353. Julich, CEC/Pergamon, New York, 1976.
25. Kelly, R., and Lam, N. Q., *in* "Ion Surface Interaction, Sputtering and Related Phenomena" (Behrisch *et al.* Eds.), p. 37. Gordon & Breach, New York, 1973.
26. Kao, C. C., Tsai, S. C., and Chung, Y. W., *in* "Metal-Support and Additive Effects in Catalysis" (B. Imelik *et al.*, Eds.), p. 211. Elsevier, Amsterdam, 1982.
27. Kesmodel, L. L., Gates, J. A., and Chung, Y. W., *Phys. Rev. B* **23,** 489 (1981).
28. Ibach, H., and Mills, D. L., "Electron Energy Loss Spectroscopy and Surface Vibrations." Academic Press, New York, 1982.
29. Soma-Noto, Y., and Sachtler, W. M. H., *J. Catal.* **32,** 315 (1974).
30. Tanaka, K., and White, J. M., *J. Catal.* **79,** 81 (1983).
31. Vannice, M. A., Twu, C. C., and Moon, S. H., *J. Catal.* **79,** 70 (1983).
32. Ichicawa, M., Fukushima, T., and Shikakura, K., "Proceedings, 8th International Congress on Catalysis, Berlin, 1984."
33. Sachtler, W. M. H., "Proceedings, 8th International Congress on Catalysis, Berlin, 1984."
34. Burch, R., and Flambard, A. R., "Metal-Support and Additive Effects in Catalysis" (B. Imelik *et al.*, Eds.), p. 193. Elsevier, Amsterdam, 1982.